ELSEVIER

Biophysical Chemistry 58 (1996) 185–204

Biophysical Chemistry

Imaging of fluorescent molecule and small ion transport through human stratum corneum during high voltage pulsing: localized transport regions are involved

Uwe F. Pliquett [a,*], Thomas E. Zewert [a], Tani Chen [b], Robert Langer [b], James C. Weaver [a]

[a] *Harvard – MIT Division of Health Sciences and Technology, Massachusetts Institute of Technology, Cambridge, MA 02138, USA*
[b] *Department of Chemical Engineering, Cambridge, MA 02138, USA*

Received 4 January 1995; revised 10 May 1995; accepted 15 May 1995

Abstract

During the application of high-voltage pulses across the skin, transport of two negatively charged fluorescent molecules through the stratum corneum is highly localized. The apparent size of these localized transport regions (LTR's) is initially 10 μm in diameter for both calcein and sulforhodamine. Appearance of LTR's occurred at or above transdermal voltages of 75 V. In the range of 75 to 160 V, the number of LTR's increases with voltage, but their initial size is the same at all voltages; with additional pulses LTR's increase in size, reaching diameters of approximately 40–80 μm. Small ion currents across the skin are also localized and include the LTR's; however, the areas of current flux appeared to be larger. There was no visible damage to the structure of the skin seen at 100 × magnification for any of the voltages used (< 170 V across the skin). Significantly, LTR's are not sweat ducts or hair follicles.

Keywords: Transdermal transport; Fluorescence microscopy; Electroporation

1. Introduction

Recently, it has been shown that the transport of small molecules such as calcein through human skin can be enhanced up to four orders of magnitude with the application of high-voltage electrical pulses [1,2]. Transport of other, considerably larger molecules, such as DNA fragments [3] and peptides [4,5] using high-field pulsing (approximately 30–500 V across the skin) has been demonstrated as well. Potential applications of this method include systemic drug delivery (e.g., pulsatile delivery of hypothalamic releasing hormones) [5], localized drug delivery (e.g., anti-sense oncogene oligonucleotides for skin tumor treatment) [3], and non-invasive sensing. The general mechanism of transport is hypothesized to be electroporation [1,6] of the outer epidermal layer, the stratum corneum, to create aqueous pathways and subsequent local transport of molecules through these pathways. In order to theoretically describe [7–9,4] and therefore predict the extent of molecular transport across the electroporated skin, knowledge of the

* Corresponding author.

SSDI 0301-4622(95)00098-4

density, distribution, fractional area and transport behavior of these pathways is expected to be essential.

Imaging of small ion transport through the stratum corneum has previously been reported by others. For example, it has been demonstrated in vivo for dry, human skin that the distribution of small ion transport is localized when an electric current is applied over the surface of the skin [10]. This author hypothesized that these localized ionic paths corre-

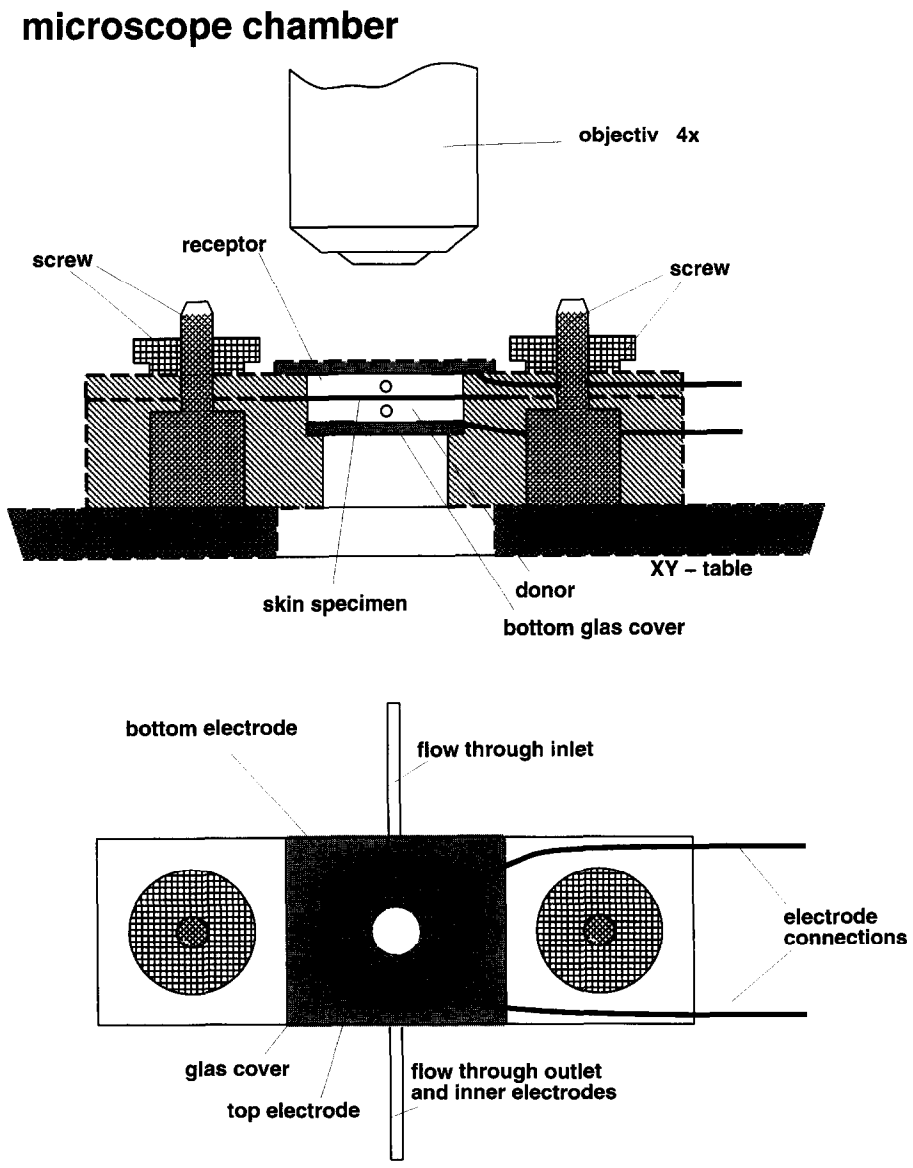

Fig. 1. Side and top view schematics of the real-time imaging apparatus. Transport of fluorescent molecules through the epidermis (stratum corneum facing down) was imaged through an Nikon stereo microscope while being pulsed in the custom chamber shown. To disperse transported molecules in the receptor compartment, and evolved gas and electrode byproducts in both compartments, continuous flow (0.5 ml/min) was maintained through the ports for both the donor and receptor compartments by a two channel peristaltic pump. During each experiment the donor solution was recycled while solution from the receptor compartment was continuously replaced with fresh saline. Fractions of the receptor solution were collected automatically and subsequently analyzed by calibrated spectrofluorimetry.

sponded to sweat ducts. In separate studies, iontophoresis through stratum corneum was shown to be localized. Specifically, discreet precipitations of prussian blue were detected by scanning electrochemical microscopy during the electrically driven transport of ferricyanide and ferrocyanide through hydrated, hairless mouse skin [11]. The most likely site of transport was identified as hair follicles. Localization of percutaneous ionic penetration was also observed in experiments in which no electrical current was applied. In that study mercuric chloride was allowed to diffuse into dermatomed human skin. When the skin was subsequently treated with ammonium sulfide, precipitated mercury was visualized with electron microscopy. For times less than one hour, it was observed that the predominant site of mercury precipitation (probable path of mercurate diffusion) was between the keratinocytes of the stratum corneum [12]. Finally, localized areas of calcein staining have been visualized by confocal microscopy in the stratum corneum after high-voltage pulses had been applied [13]. Although the results of these previous studies are important, they did not directly visualize organic molecule transport through the stratum corneum on a subsecond timescale.

Therefore, we have constructed an apparatus (Fig. 1) which allows us to image regions of molecular transport through the stratum corneum during the application of electrical pulses. In our experiments we detected negatively charged fluorescent molecules (realistic models of therapeutic agents) with a temporal resolution of approximately 0.5 s and a spatial resolution of about 2 μm. These fluorescent molecules are highly water-soluble, and do not bind significantly to the stratum corneum. Further, the experimental conditions employed were very similar to those of normal physiology (e.g., ion type, ion concentration, and pH.) We also report experiments wherein we imaged the transport of small, inorganic ions (which are responsible for almost all of the current) through the stratum corneum during electrical pulsing. With different experimental apparatuses, we detected the spatial distribution of fluorescent molecules that have been transported *through* the skin, correlating these areas with fluorescent areas of fluorescence *in* the skin; and we imaged ion transport through the skin by iontophoresis after high-voltage pulses had been applied.

2. Methods

2.1. Skin preparation

Heat-stripped stratum corneum [14] was used in all experiments, and the area of skin exposed to the electrical field was 0.7 cm^2. The skin was obtained from either the abdomen, arm, or back of adult human cadavers. Prior to heat-stripping the skin was stored at -70°C for one to six months. After heat-stripping, the skin was stored at 4°C in a 95% humidity environment. A small number of experiments with fresh skin gave similar results to those obtained with heat-stripped skin.

2.2. Fluorescent molecules

Two different water-soluble molecules were used: calcein (Molecular Probes, Eugene, OR, charge of -4, molecular weight of 623, and excitation coefficient of 0.08), which has an excitation maximum at 488 nm and an emission peak at 515 nm, and sulforhodamine (molecular weight of 607, charge of -1, excitation coefficient of 0.107) which has an excitation maximum at 586 nm and an emission maximum 607 nm. The difference in the emission spectra of the two fluorescent molecules allowed us to easily distinguish them.

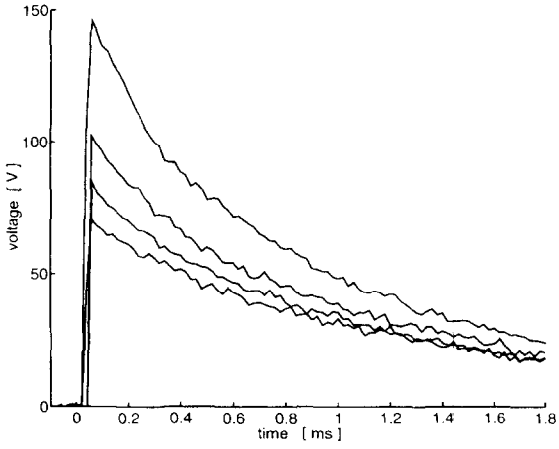

Fig. 2. Trace of voltage across the skin (U_{skin}) during application of exponential pulses (at the pulser output, U_{pulser}) of 250, 500, 1000, 1500 V (from bottom to top trace).

2.3. Fluorescence imaging apparatus (Fig. 1)

The chamber was fabricated from acrylic. The lower part of the chamber (donor compartment) was filled with pH 7.4 phosphate-buffered saline (PBS) (Sigma, St. Louis, MO), and 1 mM calcein and/or 1 mM sulforhodamine. The upper part (the receptor compartment) was filled with PBS. The donor compartment contained PBS, 3–5 mM methylene blue, and 1 mM of sulforhodamine and calcein. The methylene blue was added to absorb emitted light from the fluorescent molecules in the donor compartment

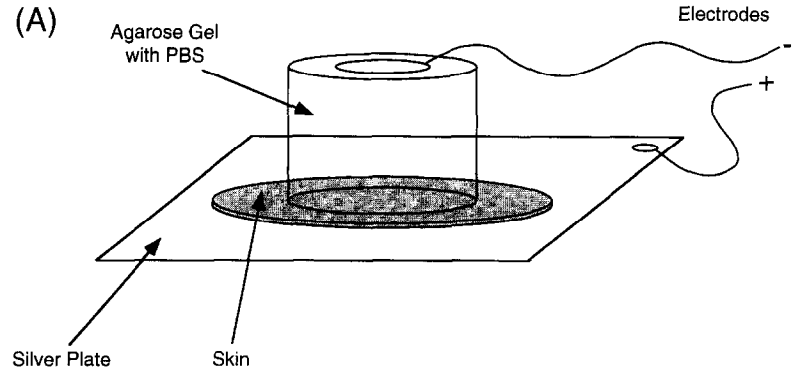

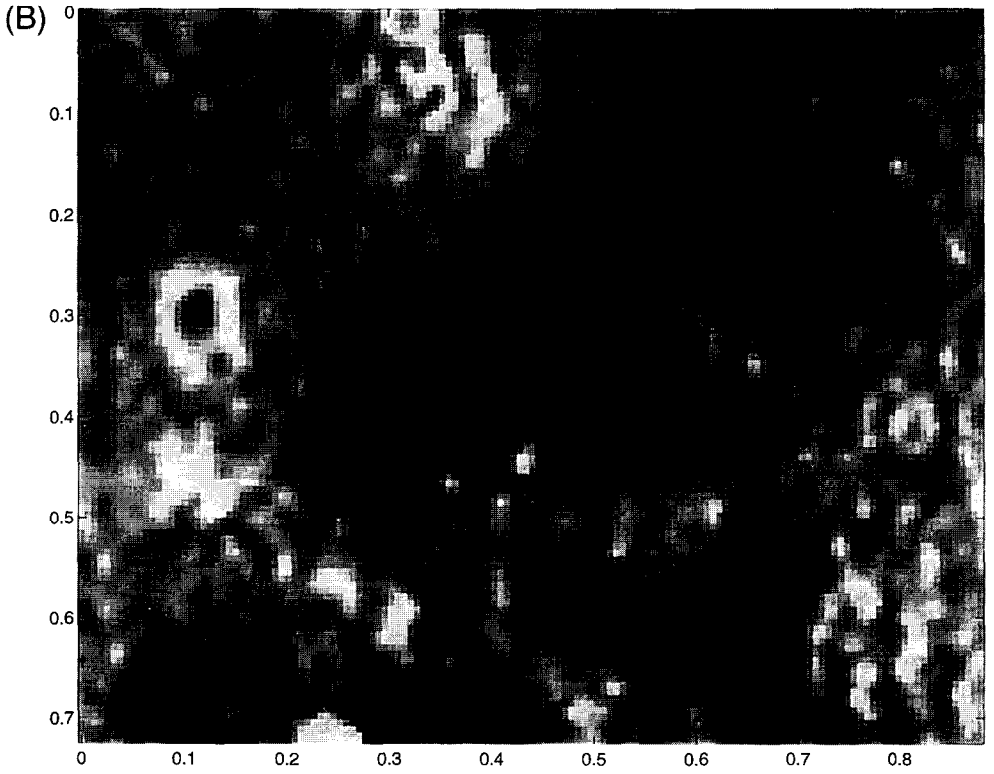

Fig. 3. (A) Schematic used for the imaging of the ionic pathways after pulsing was completed. (B) Image of the ionic pathways (Cl^--ions) as dark region at the silver plate.

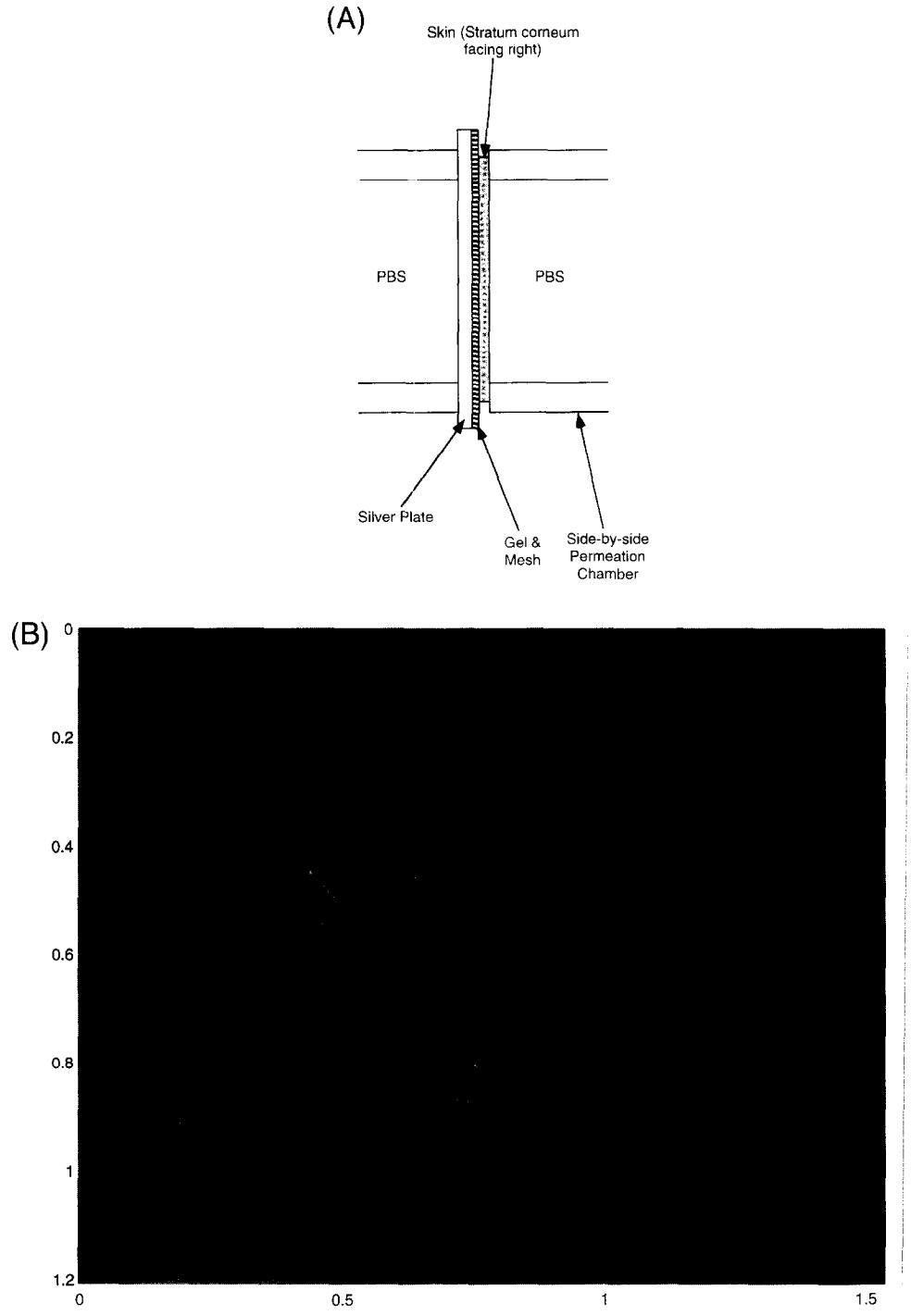

Fig. 4. (A) Composition of the gel-sandwich used for the imaging of molecules crossing the stratum corneum. (B) Retained red fluorescence in the agarose gel. This result provided evidence that the LTR's are the site of transport, not just internal skin staining. (We do not show data for calcein as it diffuses through the agarose gel much more quickly and the mesh shows a week but visible autofluorescence in the green range).

solution. The skin preparation is only 50 μm thick and thus transmits visible light. Such background light obscures visualization of fluorescent molecules that have passed through the stratum corneum. Black filter paper (mixed cellulose ester, 0.45 μm pore, Millipore) placed on the donor side next to the stratum corneum further diminished background fluorescence. A positive pressure of 100 mm H_2O in the receptor compartment relative to the donor compartment was maintained so that the skin was pressed flush against the filter paper.

For the application of the electric field one electrode was provided in each compartment. The top electrode was a stainless steel sheet located 3 mm away from the skin and with an optical window of 0.35 cm^2 for the observation of the skin. The bottom electrode was a silver disc, also 3 mm from the skin. The donor compartment was at the negative and the receptor compartment at the positive side of the pulser. This 'forward direction' polarity provided an electrophoretic driving force through the skin for the negatively charged fluorescent molecules. However, methylene blue is positively charged so that the driving force for its transport was away from the skin. Thus, this specialized apparatus provided both pulsing and optical conditions compatible with real time imaging of fluorescent molecule and small ion transport.

2.4. Pulse application and electrical measurements

High-voltage pulses were delivered using an exponential pulser (GenePulser, BioRad, Richmond, CA) modified for computer control. To fix the time constant an external voltage divider (10 Ω:40 Ω, noninductive, 50 W) was used, with the chamber connected across the 40 Ω-resistor. The pulse time constants were $t_{pulse} = 1.0 \pm 0.1$ ms.

For current (I) measurements an additional 5 Ω resistor was placed in series to the chamber, and voltage trace across it was stored in an digital oscilloscope (Hewlett Packard-54601) for subsequent calculation. The inlets of the donor and the receptor compartments were fabricated from an 18 gauge stainless steel needle so that these ports could also be used as electrodes over which an 'inner voltage' (U_{inner}) drop was recorded. The distance between these electrodes was 2.4 mm, and the resistance of the solution (R_{sal}) between them was 20.6 Ω. This inner voltage drop across these electrodes was also stored in the digital oscilloscope (other channel), so that the transdermal voltage (U_{skin}) could be calculated from

$$U_{skin} = U_{inner} - IR_{sal}.$$

In the figures and text we generally refer to U_{skin} rather than the voltage applied at the electrodes, as this is relevant to the transport mechanism. The results of such calculations are displayed in Fig. 2.

2.5. Image acquisition

A fluorescence microscope (Nikon Labophot-2 with Planapo Optics) was used, together with a video imaging system, based on a Nikon FX-35DX camera and a Macintosh Quadra 950 computer. For general image storage we used a video reorder (Toshiba M-448). Otherwise, images were gathered directly using the IPLab Spectrum program (Signal Analytics Co.), and the data were transferred to a Sun Sparc 10 workstation as TIFF files for subsequent computation. When photographic images were recorded, shutter times between 1/4 and 3 s were used. For advanced image acquisition, such as shown in Fig. 8, a Sony X-1744 video camera was used with an integration time of 1/2 s which allowed a preprocessing of the frame.

Fig. 5. Fluorescence images of local transport regions (LTR's) for (A) calcein based on green fluorescence, and (B) sulforhodamine based on red fluorescence. These images were obtained following completion of a multiple phase protocol (see methods section). These images were directly taken by IPLab through the optics described. The bright nearly circular areas of fluorescence are LTR's (see text). These green and red fluorescence images were obtained simultaneously; but the green and red fluorescence from calcein and sulforhodamine are processed separately. Note the general coincidence of green and red fluorescence. The calcein fluorescence highlights the structure of the skin more. The long dark lines in (A) correspond to the Rete pegs (valleys) of the skin. One can also see the outlines of some polygonal keratinocytes with diameters of approximately 40 μm. The LTR's appear to involve one or a few keratinocytes. Throughout the pixel size is 2×2 μm.

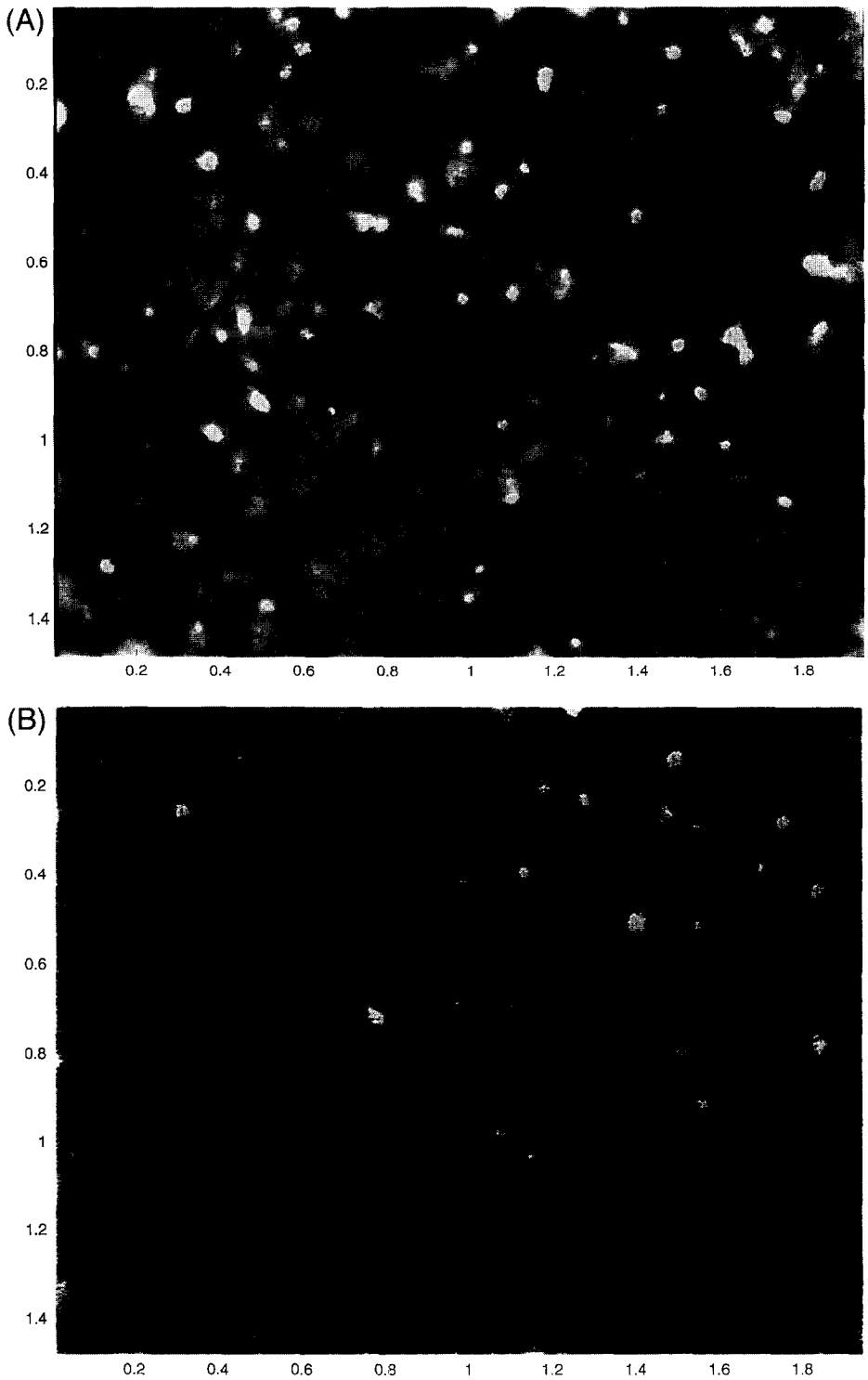
(A)
0.2
0.4
0.6
0.8
1
1.2
1.4
0.2
0.4
0.6
0.8
1
1.2
1.4
1.6
1.8
(B)
0.2
0.4
0.6
0.8
1
1.2
1.4
0.2
0.4
0.6
0.8
1
1.2
1.4
1.6
1.8

2.6. Imaging of small ion transport regions

Because ions are not typically visible by fluorescence, we used a chemical reaction, the reaction of chloride anion with the silver cation created at the anode surface, to visualize the sites of current due to these ions. A transparent polystyrene plate was coated with silver using Tollen's reagent [15]. The surface resistivity of this electrode was found to be substantially smaller than the other components in the system. This electrode was placed directly in contact with the skin surface. Sites of current through the skin corresponded to areas of corrosion (silver chloride formation and solubilization) of the thin silver electrode. Light transmitted through these areas could then be recorded in real time using a video imaging microscope. To examine regions which retained transport ability for a long time (up to several hours) after pulsing, we removed the skin from the apparatus in Fig. 1 and then placed it on a polished silver surface with the stratum corneum side touching the surface. A 5 mm thick agarose disc (made with 2% agarose in PBS) connected to a negative electrode was placed on top of the skin, with the polished silver serving as the positive electrode. The agarose disc was smaller than the skin preparation to avoid shunting pathways around the skin (Fig. 3A). For 30 s a current of 1 mA (1.4 mA/cm^2) was used and after this the gel disc was removed. Under the fluorescence microscope the sites of transdermal, molecular transport that had formed during experiments with the apparatus in Fig. 1 were still visible. By changing the illumination to white light, the sites of cumulative current flow during the iontophoresis were visible as dark zones on the silver electrode (which could be seen through the skin). A better view of the anion deposition at the silver surface was provided after removing the skin from the silver electrode (Fig. 3B). Subsequent computer analysis was performed to determine the degree of the coincidence between localized transport regions (LTR's) of fluorescent molecules during pulsing and regions of small ion transport after the pulsing.

2.7. Fluorescent molecule transport across the stratum corneum

To determine the net transport of fluorescent molecules we used an automatic sampling system to collect aliquots of the receptor stream. The brightness of these aliquots was measured after the experiment using a spectrofluorimeter (Fluorolog 2, model F112AI, SPEX Industries, Edison, NJ). These measurements provided assurance that the total molecular transport was comparable to that in many previous experiments. To visualize sites of local transport, we coated a silver sheet electrode (anode) with agarose (0.2 mm thick). The stratum corneum side of the skin preparation was then placed in contact with the agarose side of the electrode so that any fluorescent molecule transported could be retained temporarily. To maintain the distance between gel and the electrode and hinder the lateral diffusion of fluorescent molecules, a nylon mesh (50 μm spacing) was placed inside the gel. This set up was placed into a side-by-side chamber with a PBS donor solution (1 mM fluorescent molecule) on the other side (Fig. 4A). Pulsing was applied between the silver plate (cathode) and a Ag/AgCl electrode (anode) placed in the donor compartment. Usually 10 pulses with one minute spacing were provided with a voltage across the electrodes (U_{pulser}) of 1000 V. The electrode/agarose/skin slab was then removed from the chamber and placed under the fluorescence microscope. Photomicrographs were taken of the layers together and separately. Under the appropriate excitation wavelengths fluorescence from molecules in the agarose and skin could be seen; and under white light, staining of the silver electrode due to ion deposition could also be seen.

3. Results

The most striking result is that transport of calcein, sulforhodamine, and small ions are all highly localized. In the case of fluorescent molecules we observed that transport of calcein and sulforhodamine was localized to regions whose initial size is about 10 μm in diameter (width at half-maximum) when pulses of 75 V or higher occur across the skin. The smallest bright spots seen in Fig. 5A and 5B, and the smallest contours in Fig. 6 are images of these areas. The diameters of these localized transport regions (LTR's) quickly (in tenths of seconds) enlarge to as great as 50 μm, presumably due to lateral diffusion or continued driven transport out of

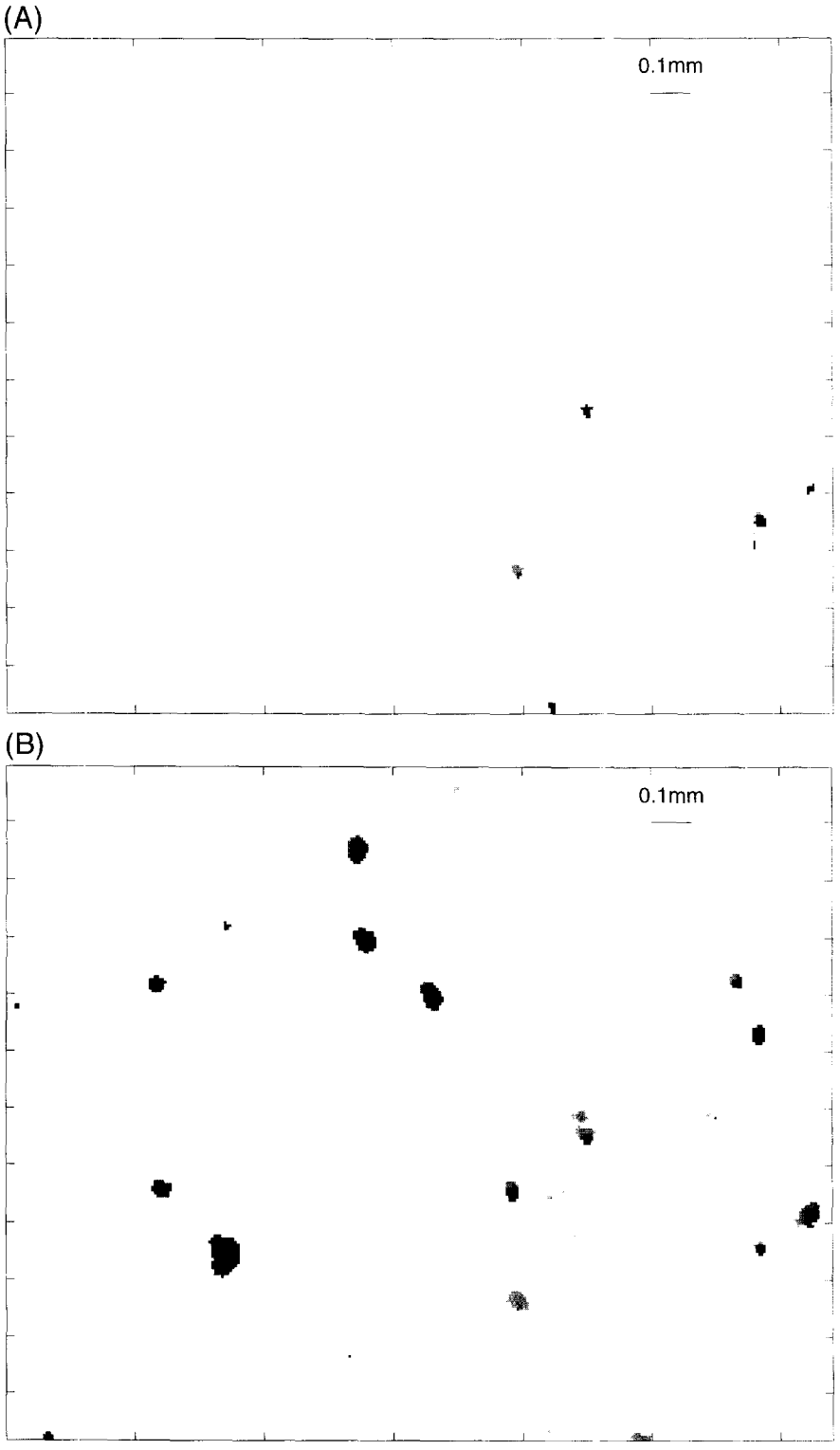

(Continued overleaf)

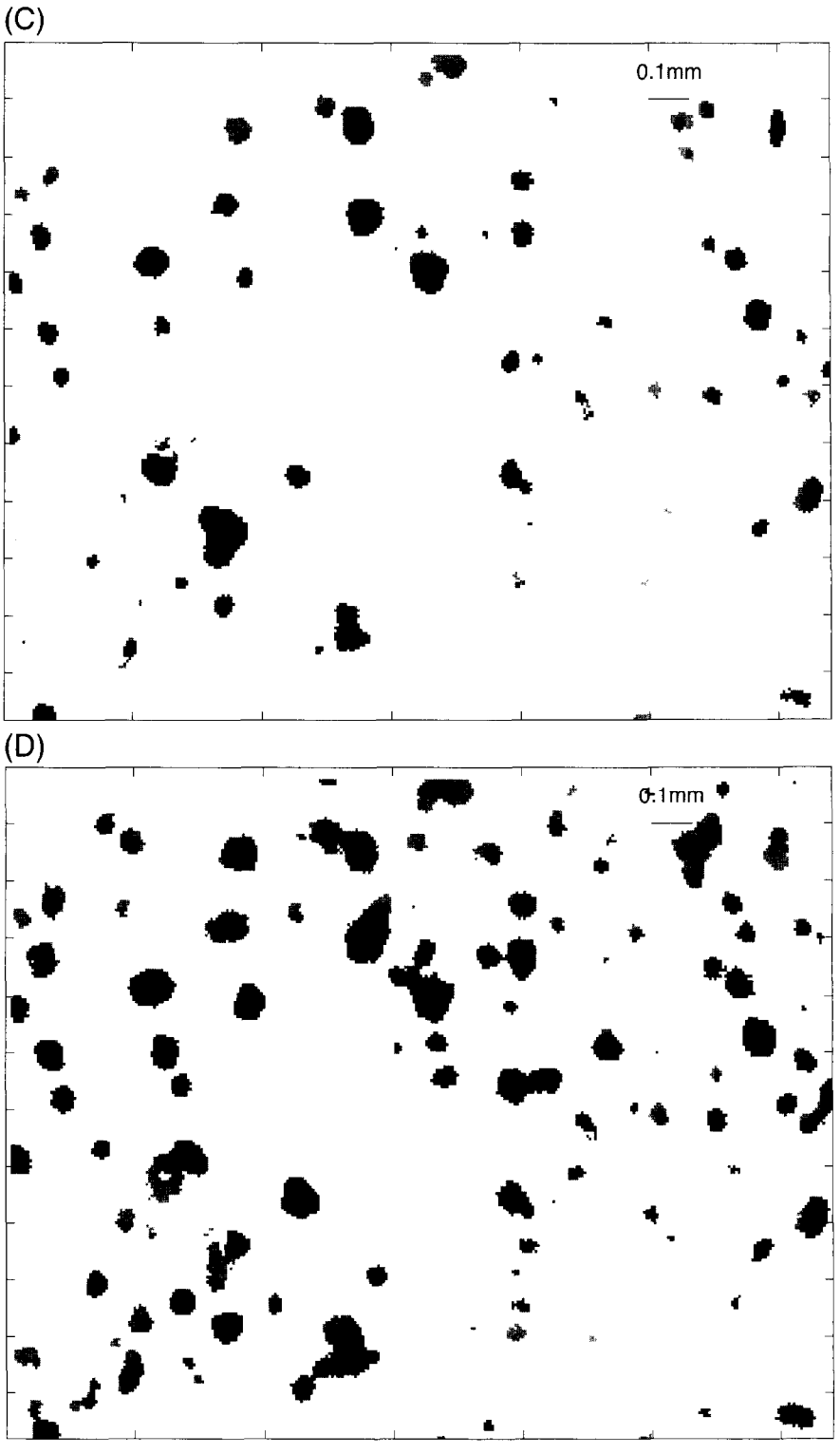
(C)
0.1mm
(D)
0.1mm

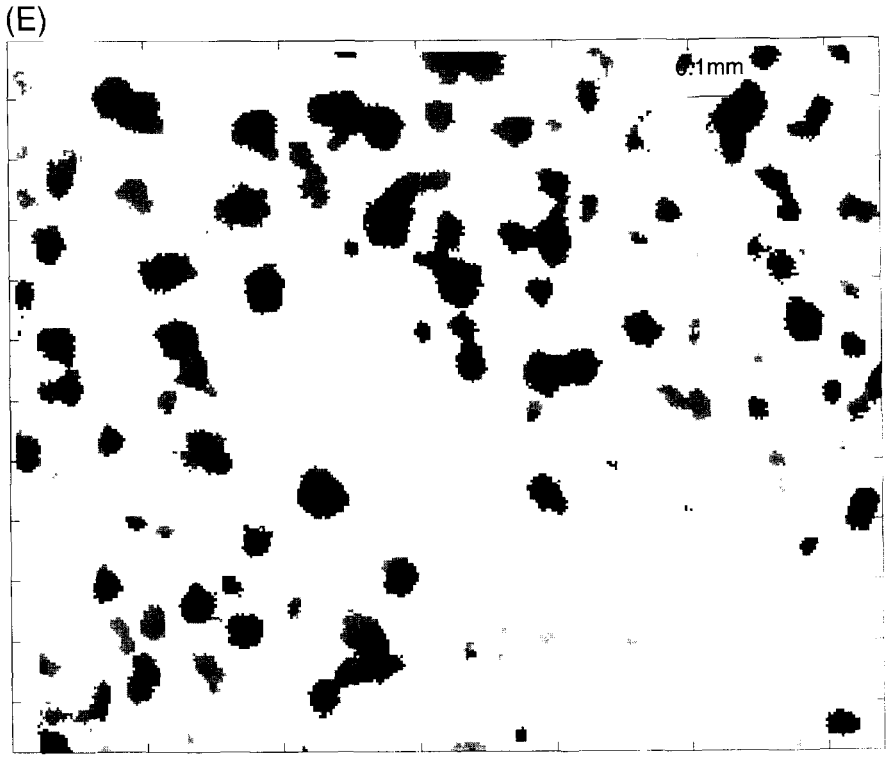

Fig. 6. Contour plots of images of calcein and sulforhodamine transport through the skin after different voltages and numbers of pulses. The lighter hatching represents areas of calcein only transport, the darker hatching represents areas of sulforhodamine only transport, and the black regions represent coincident areas of calcein and sulforhodamine transport after (A) 75 V three pulses; (B) 75 V, ten pulses and 99 V, three pulses; (C) 75 V ten pulses, 99 V ten pulses, and 120 V, three pulses; (D) 75 V ten pulses, 99 V ten pulses, and 120 V, ten pulses, and 160 V, three pulses; (E) 75 V ten pulses, 99 V ten pulses, and 120 V, ten pulses, and 160 V, ten pulses. These contours were computed from video camera images, using an average of four frames. The transport through a single skin preparation is represented in this figure. The new LTR's which appear with each successive image are much greater on average than 10–20 μm of initial LTR's referred to in the text, because these plots were made from the images obtained after the third pulse following a voltage increase. For this reason significant lateral dispersion had occurred. The cut-off of the contour is 40% of the maximum brightness obtained in that image, and was computed separately for calcein and sulforhodamine. In (A) the smallest LTR's are the newest LTR's, that is, those that arose after the last few pulses. Although the average size of the LTR's becomes larger with increasing number of pulses and voltages, new LTR's appearing just after each increase in voltage with approximately the same size.

the LTR after the pulse. When viewing the evolution of LTR's directly through the microscope in real time, however, human observers estimated the diameter to be even smaller (approximately 5 μm). We are not certain whether this discrepancy in the measurement of the size of the initial LTR's is due to lateral transport before an image could be acquired, or instead a perceived contrast by the observer at very high values of the intensity of the spots. Fig. 7A and 7B shows a more magnified image and a three-dimensional plot (Fig. 7C and 7D) of the fluorescence intensity of these regions as they appear following a single 76 V pulse applied across the skin. In our experiments, the small, incipient stage of fluorescence localization is more difficult to distinguish for the larger pulses because in our protocol a series of pulses of increasing voltages was used. As a result background fluorescence builds up in the skin from previous pulses at lower voltages.

Fig. 8A shows that an LTR contains several subpeaks that are not discernible by simple inspection. This computer-generated representation was taken after the application of more than 30 pulses. Signal averaging revealed subpeaks which are not visible by

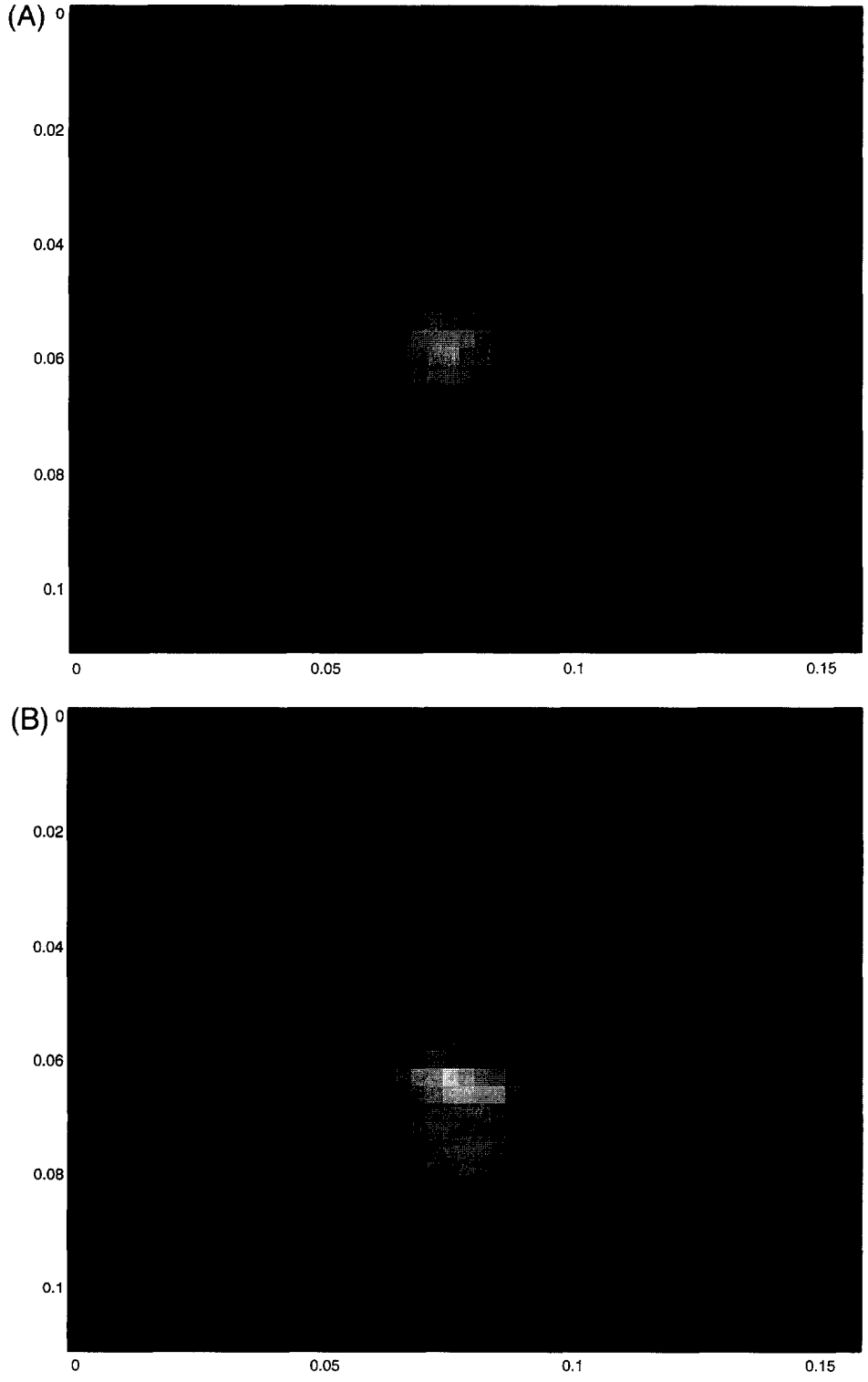
(A)
0
0.02
0.04
0.06
0.08
0.1
0
0.05
0.1
0.15
(B)
0
0.02
0.04
0.06
0.08
0.1
0
0.05
0.1
0.15

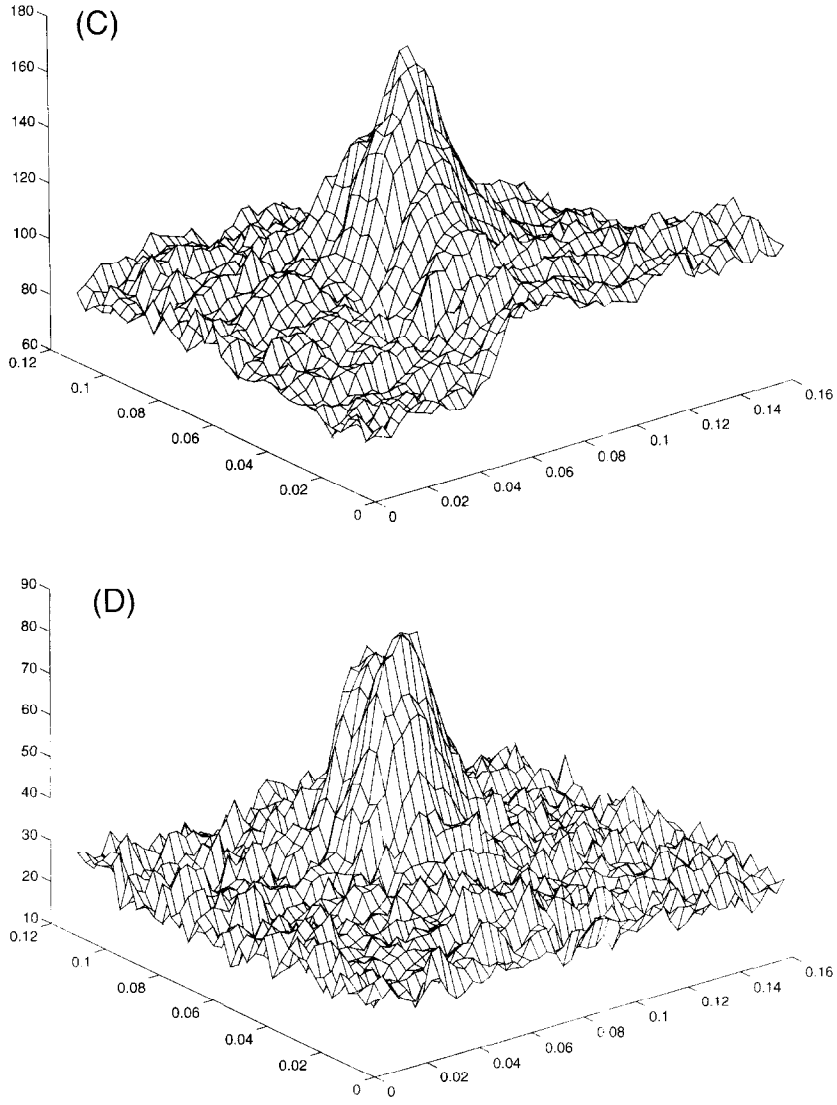

Fig. 7. Magnified image of an LTR for (A) calcein fluorescence and (B) sulforhodamine fluorescence after a single pulse at 76 V (U_{skin}). This is a magnified view of one LTR analyzed for calcein and sulforhodamine brightness. This is the earliest stage at which we could capture an image of an LTR, but it has already laterally spread somewhat. The image was directly acquired through IPLab from the microscope. (C) and (D) are expanded three-dimensional plots of fluorescence in arbitrary units for brightness (vertical axes) of the corresponding regions of (A) and (B), respectively. Both the x- and y-axes of (A) and (B) give position in millimeters. The numbers of these axes correspond to the in the x- and y-axes of (C) and (D). The width at half-maximum of the peaks in (C) and (D) is approximately 10 μm, a value consistently found for the earliest visualized stage of LTR development.

simple observation under the microscope in LTR's that had already spread out laterally. As shown in Fig. 8B, the diameters of the subpeaks are approximately 10 μm, and a single LTR consists of about 10 different subregions. The significance of these substructures are not yet understood.

During high-voltage pulsing LTR's for both calcein and sulforhodamine are distributed with apparent randomness over the stratum corneum topography (Fig. 5A and 5B), but there are two major exceptions: (1) No LTR's were found in the valleys (Rete pegs) of the stratum corneum. (2) Although

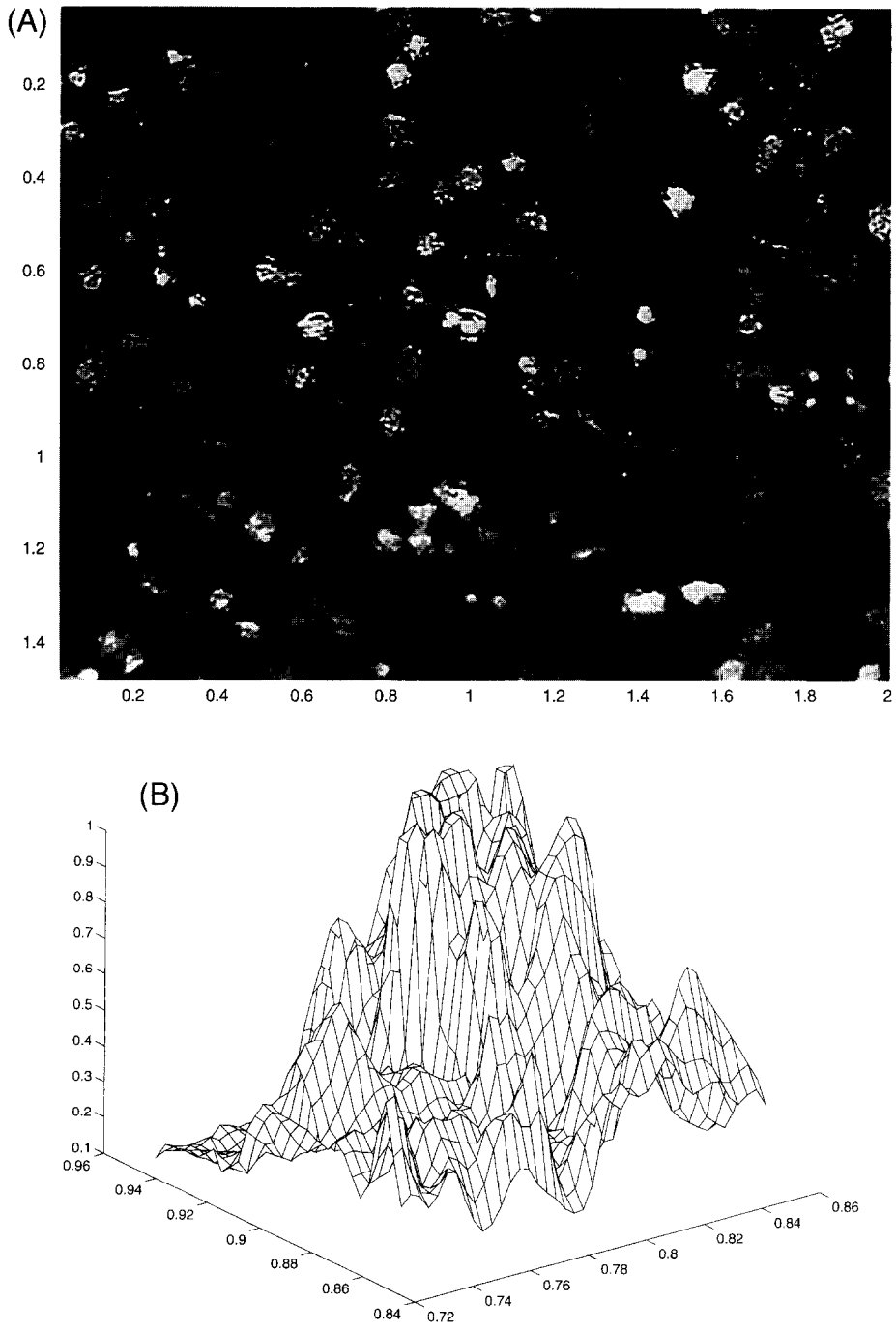

Fig. 8. Signal-averaged image of LTR's from a calcein fluorescence image of a skin preparation which had been pulsed ten times at 157 V (U_{skin}). The averaging was carried out using a special camera (Sony X-1744). The x- and y-axes of (A) and (B) are in millimeters and correspond. The z-axis of (B) is in arbitrary fluorescence units.

calcein (the more charged molecule) staining of the appendages (hair follicles and sweat ducts) occurs, the LTR's do not correspond to appendages. Also, very little sulforhodamine (the lesser charged molecule) fluorescence is seen in the appendages. These observation hold for all pulsing voltages at which we observed transport.

Pulsing below 75 V, no localized fluorescent molecule transport was detected by fluorescence microscopy of the skin. This result is consistent with previous work in that significant molecular transport does not occur below this voltage for ten pulses of one millisecond time constant [16]. As the pulsing voltage across the skin is increased above 75 V, the number of LTR's increases significantly for both fluorescent molecules (Fig. 9); however, the average size of each new LTR formed is the same as the average size (about 10 μm) of the LTR's originally formed at the lower voltages. New LTR's are primarily formed after the first pulse at a higher voltage. Typically, one tenth as many new LTR's are formed by the second pulse at a given voltage, and only rarely are new LTR's formed after the third or subsequent pulses at a given voltage. Continued pulsing at a constant voltage results in more transported molecules in an LTR. The fluorescence then spreads laterally and may merge (or create the appearance of merging) with another LTR. This behavior is also apparent in the contour plots of a typical sample in Fig. 6, and from the graph of the average total area of LTR's computed from 14 skin preparations (Fig. 10).

A generalized analysis of the images of several transport LTR's from many skin samples is presented in Fig. 11. As shown, the calcein LTR's exhibited increasing green fluorescence background and peak width with continued pulsing. The maximum green fluorescence increases at higher voltage pulses but stays the same with pulsing at the same voltage. For the same LTR's the sulforhodamine (red fluorescence) background increases with continued pulsing at the same and/or higher voltages, but the increase is smaller than for calcein, especially with respect to continued pulsing at the same voltage. The sulforhodamine LTR's broaden with increased pulsing at the same and/or higher voltages even more than for calcein. (For calcein the width at half maximum is 30 μm for the first curve and 60 μm for the last; whereas, for sulforhodamine the corresponding values are 30 μm and 90 μm). The increase in maximum brightness occurs in going up to 118 V but does not occur in going from 118 to 158 V.

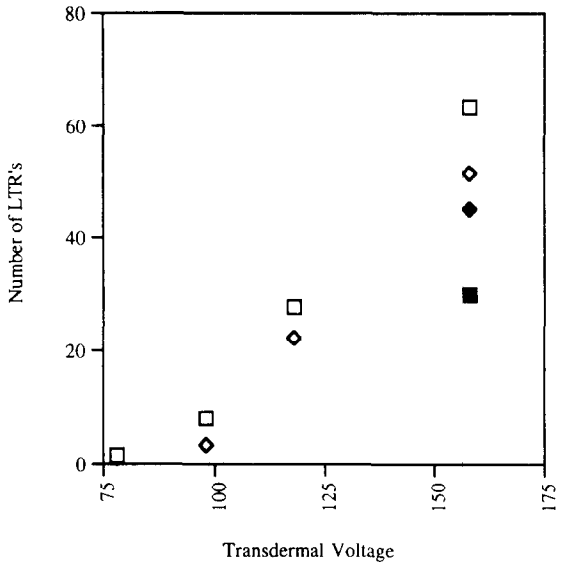

Fig. 9. Plot of the number of LTR's for calcein (squares) and sulforhodamine (diamonds) as a function of voltage and pulse number across a 0.7 cm^2 skin preparation. Light-bordered squares are one pulse calcein, bold square is ten pulses calcein; light-bordered diamonds are one pulse sulforhodamine; bold diamond is ten pulses sulforhodamine at the indicated transdermal voltages. These data are an average of 14 skin samples. Note that at each voltage, ten pulses at each lower voltage has previously been applied. The threshold for including an LTR is 40% of the maximum fluorescence in an image. The number of calcein LTR's is always greater than the number of sulforhodamine LTR's after one pulse at a given voltage. For both fluorescent molecules the number of LTR's increases with increasing voltage. However, the number of LTR's decreases for both fluorescent molecules when the skin was pulsed at a 158 V ten times compared to when the skin was pulsed at this voltage only once. Moreover, the number of LTR's visualized with calcein decreases to less than half of its original value when pulsed ten times at 158 V, whereas, for sulforhodamine the decrease in the number of LTR's from one to ten pulses is not statistically significant. Also, after ten pulses at 158 V, the number of LTR's visualized with sulforhodamine is greater than the number visualized with calcein. The lateral spread of calcein was greater than for sulforhodamine when a several pulses are applied at the same voltage. The number of calcein LTR's appears to decrease because the background of calcein increases and the calcein LTR's merge due to broadening of their fluorescence profiles. Sulforhodamine LTR's decrease less in number because there is less background increase (Fig. 5). Some LTR's merge due to broadening.

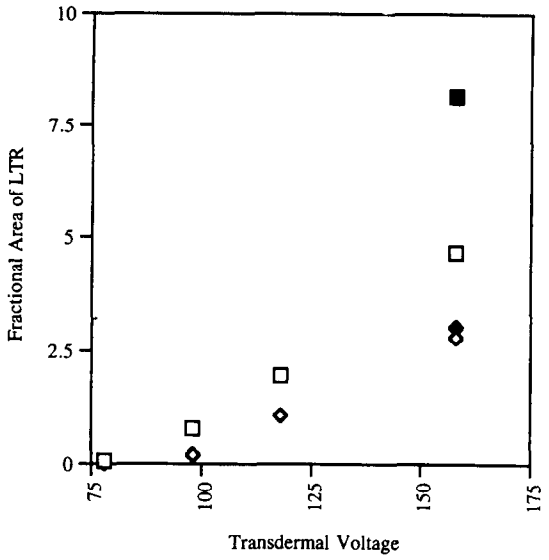

Fig. 10. Plot of the fractional area of skin occupied by LTR's formed for calcein and sulforhodamine transport as a function of transdermal voltage. The parameters, images, and symbols are those of Fig. 9. The dependence is similar to that of Fig. 9. After ten pulses the fractional area increases for both calcein and sulforhodamine, but the increase compared to one pulse is statistically insignificant for sulforhodamine. In contrast, the increase is for calcein is substantial. Considering that the number of LTR's after one pulse is greater than the number of LTR's after ten pulses for calcein (Fig. 7), this result clearly demonstrates the greater lateral spreading for calcein.

Interestingly, the maximum red fluorescence brightness actually decreases in going from three to ten pulses at 158 V.

Real time transport of small ions was also observed (Fig. 9) by using a silver-coated polystyrene plate (anode) that was in direct contact with the stratum corneum. In this case we used the apparatus of Fig. 1, but with the receptor compartment replaced by the thin silver-coated electrode. After the application of 1000 V electrical pulses (the transdermal voltage is much less, but we could not determine it in this experiment because no inner electrodes were present), the silver film electrode corrodes and becomes transparent. With further pulsing at this voltage still larger areas of transparency were created. For example, over 50% of the surface became transparent after three pulses of 1000 V across the electrodes. These areas of transparency are caused by the reaction of ions (presumably, chloride) with the

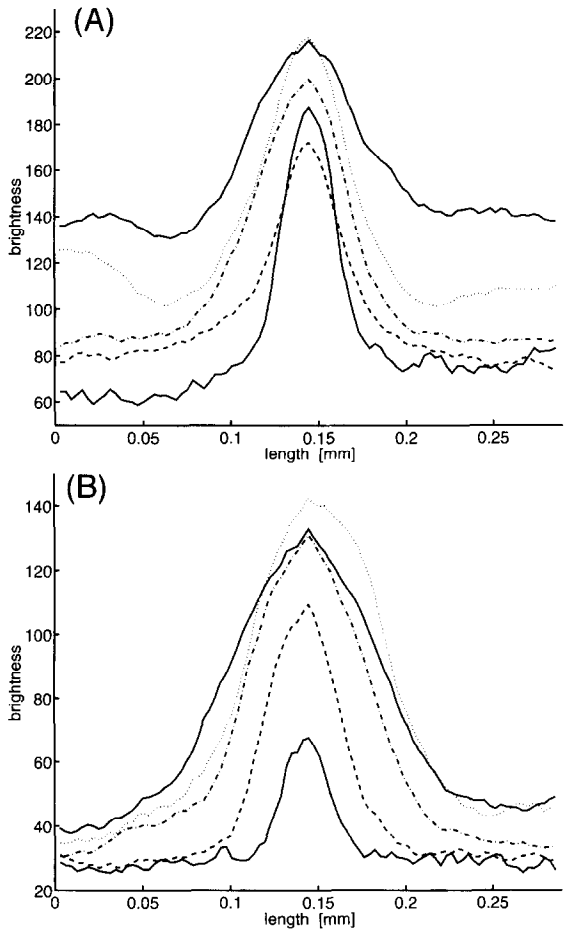

Fig. 11. Graph of the average fluorescence of cross-sections through several images of LTR's after pulsing at different voltages. To generate these plots two-dimensional fluorescence profiles of LTR's were constructed, and then aligned by their maximum brightness for each condition (i.e., number and voltages of pulses). An average fluorescence profile was then obtained for each condition. These averages for calcein (A) and sulforhodamine (B) brightness for different pulsing conditions are displayed. The bottom curves in (A) and (B) represent the average brightness for the same four LTR's in a skin sample after having been pulsed three times at a transdermal voltage of 76 V. The remaining four curves in (A) and (B) represent the average brightness of twenty LTR's from a skin sample as are pulsed with progressively higher voltages. From the bottom of the graphs up: (—) average of four points 78 V, three pulses; (----) average of twenty points, 78 V, ten pulses and 98 V, three pulses; (·····) average of twenty points, 78 V ten pulses, 98 V ten pulses, and 118 V, three pulses; ("""") average of twenty points, 78 V ten pulses, 98 V ten pulses, and 118 V, ten pulses, and 158 V, three pulses; (—) average of twenty points, 78 V ten pulses, 98 V ten pulses, and 118 V, ten pulses, and 158 V, ten pulses.

silver associated with current through the stratum corneum, and therefore provide a contrast mechanism based on cumulative small ion transport.

The existence of ionic transport pathways which persist after pulsing was observed in yet another set of experiments. By placing the treated skin specimen from the pulsing chamber into the apparatus as in Fig. 3A we detect the ionic pathways by AgCl deposition at the polished silver surface. Anions (mainly, chloride and phosphate) reacted with the anode after presumably having traversed the skin (Fig. 3B). These areas of localized anion current density remain accessible to iontophoresis on the time scale of hours, even though these experiments were typically done within minutes after pulsing. With the silver electrode still attached to the stratum corneum we were able to compare areas of molecular transport (fluorescent areas) and the ionic transport (dark areas at the silver surface). We generally observed that the areas of fluorescent molecule and current flux coincided, with the latter being larger. We are as yet unable to accurately record these images because the glare from the silver surface below the skin prohibits us from imaging fluorescence in the skin.

Establishing a relationship between localized skin fluorescence and actual transport is important. To this end, we temporarily retained the fluorescent molecules crossing the stratum corneum by using an experimental arrangement, with an modified standard side-by-side permeation apparatus (Fig. 4A) [17]. The agarose gel–mesh allowed temporary retention of the fluorescent molecules which crossed the skin and entered the gel–mesh layer (Fig. 4B). Our interpretation is simple but fundamental: fluorescent molecules found to be retained in the gel–mesh had to have come through the skin at the adjacent site. We found a very good agreement between areas of calcein and sulforhodamine fluorescence in the skin and in the agarose gel. The areas in the gel layer (Fig. 4B), however, were much broader than those in the skin (Fig. 5B), presumably due to lateral diffusion within the gel. In some cases a stained region in the stratum corneum did not correspond to the staining in the gel, but a stained region in the gel always corresponded to a stained region in the stratum corneum. Little staining of the agarose occurred at regions corresponding to sweat ducts and hair follicles indicating that relatively few molecules had been transported through these structures. Finally, we found that fluorescent LTR's in the stratum corneum corresponded well to dark regions at the silver surface, indicating that small ion transport occurs preferentially in the LTR's.

4. Discussion

Our basic interpretation is that the regions of strong green and red fluorescence correspond to areas of transport across the stratum corneum. From the concentration of the fluorescent molecules in the sample stream (data not shown) and from many previous experiments, [16,18] it is known, that significant transport of molecules occurs during high-voltage pulsing. The apparatus in Fig. 1 allowed imaging of localized fluorescence during pulsing. One might argue that the localized fluorescent regions are not permeable but trap fluorescent molecules instead, and that the transport occurs within the rest of the unstained surface. The counter explanation is, that the transport occurs at the stained sites, leaving a fluorescent trace behind. The agarose gel layer experiments allowed us to definitively distinguish between these two possibilities. Namely, we never found fluorescent molecules trapped in sites of the agarose where the skin was unstained, but we did find fluorescent molecules in the agarose corresponding to the regions in the skin that were stained. The temporary retention of fluorescence in the gel is direct evidence for transport across the skin. Thus, these observations strongly support the conclusion that the fluorescent sites which evolve in the stratum corneum at the moment we apply a high-voltage pulse are regions of fluorescent molecule transport through the entire stratum corneum. For this reason we refer to these fluorescent areas in the pulsed skin as localized transport regions (LTR's).

It is usually reported that significant ion transport during iontophoresis occurs primarily through the appendages [19]. However, our observations clearly demonstrate that transport during high-voltage pulsing occurs primarily in the LTR's which do not correspond to appendages. Specifically, examination under fluorescence detection conditions and with white light between pulses confirmed the fact that

the LTR's are not appendages. Further, the transport-confirming experiments using agarose gel in the receptor compartment revealed that although some calcein fluorescence corresponded to appendages, the intensity was considerably less than that corresponding to a typical LTR (indicating less calcein transport per appendage than in a typical LTR). Further, no sulforhodamine staining was observed in appendages in the skin or in areas of agarose corresponding to appendages, but significant sulforhodamine fluorescence was found in regions within the agarose layer corresponding to LTR's.

In the experiments with AgCl deposition during post-pulse iontophoresis, the deposition corresponding to the LTR's was in general greater (i.e., areas were darker) than the deposition behind the appendages. Since the apparent fractional areas of the LTR's from this experiment and the fluorescence experiments were typically 1–10% (for transdermal voltages > 80 V) while the fractional area of the appendages is 0.1%, we conclude that the LTR's are the major source of current transport during post-pulse iontophoresis.

LTR's were always located in the area of the heat-stripped skin corresponding to the dermal papillae (troughs of the epidermis) and no LTR's appeared in the Rete pegs (crests of the epidermis). We do not presently have an explanation for this finding. Examining the skin after pulsing, we also observed that after lower-voltage pulses (< 80 V) the edges are have more red and green fluorescence than the interiors of the keratinocytes in the LTR's; whereas, after higher voltage pulses (> 160 V) the fluorescence of the edges and interiors of the keratinocytes are indistinguishable (data not shown). These results are in agreement with confocal microscopy observations after pulsing [13]. An interpretation consistent with these findings is that high-voltage pulsing creates aqueous pathways that pass through the keratinocyte, i.e., electroporation of stratum corneum lipid barriers occurs.

After the first appearance of an LTR, it spreads

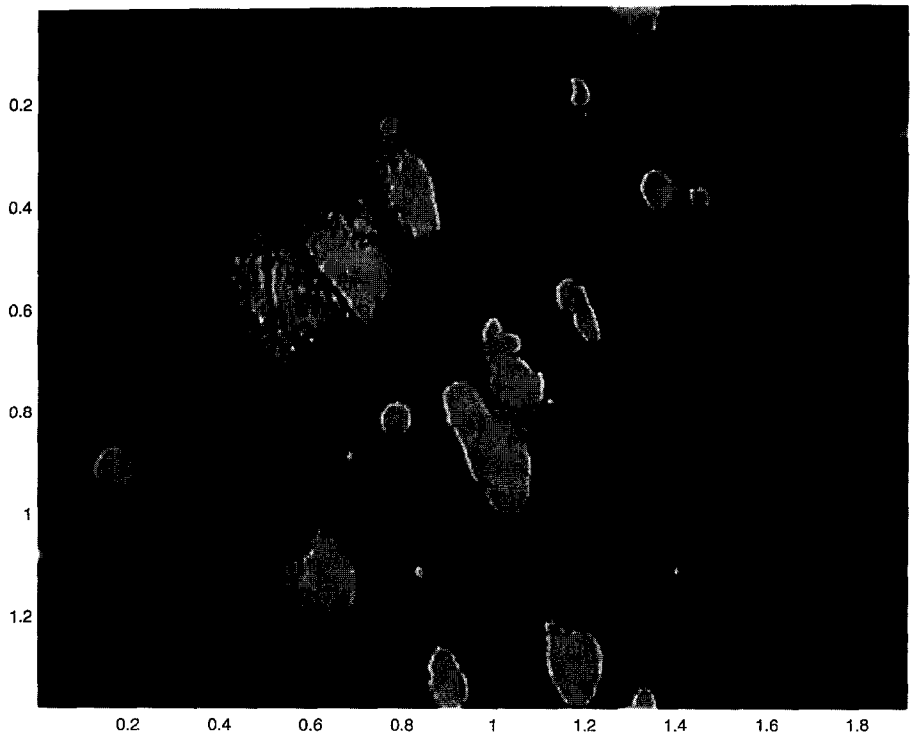

Fig. 12. Image through a thin silver electrode (anode) immediately after pulsing of the stratum corneum once with an applied electrode voltage of 1000 V (not U_{skin}) and a time constant of 1 ms.

out in less than a second from 10 μm to approximately 50 μm. With subsequent pulses at low voltages, it gains brightness and spreads further. With the application of pulses of higher voltage, the LTR spreads out to about 40–80 μm and on average the maximum brightness remains constant (Fig. 6). However, if we examine this average more closely, we find a significant variability in the fate of LTR's. For example, the fluorescence of some LTR's diminishes to the level of background, new LTR's appear in close proximity and then overwhelm the brightness of the older LTR. Eventually, the area corresponding to the maximum in brightness of the old LTR actually decreases in intensity (Fig. 12A).

One possible explanation of this phenomenon is that once an LTR is active, its dynamic resistance decreases with subsequent pulsing (Fig. 13). This interpretation is consistent with two facts: (1) it is known from this study that the number of LTR's created after the third pulse at a constant voltage increases very little; whereas, (2) it is known from previous work that the dynamic resistance of the skin decreases with continued pulsing at a constant voltage [6]. As a consequence, the voltage across the LTR will decrease with subsequent pulsing. Although the characteristic diameter (10 to 80 microns) of an LTR is much larger than that of the transient aqueous pores that are believed responsible for single membrane bilayer electroporation, the local transdermal voltage is expected to decrease because of a voltage divider effect involving the interior pore resistance and the spreading (access) resistance which involves inhomogeneous electric fields near the entrance and exits of the pores [20,21]. In contrast, the voltage of the surrounding area will be less affected. After a certain number of pulses, the voltage across the LTR is no longer great enough to reopen it after the recovery of resistance which occurs after that pulse. The resistance around the surrounding area increases even more as there is no shunting of current around the 'old' LTR. Once these 'new' LTR's proximal to the 'old' LTR are created, the current will be shunted from the area of the 'old'

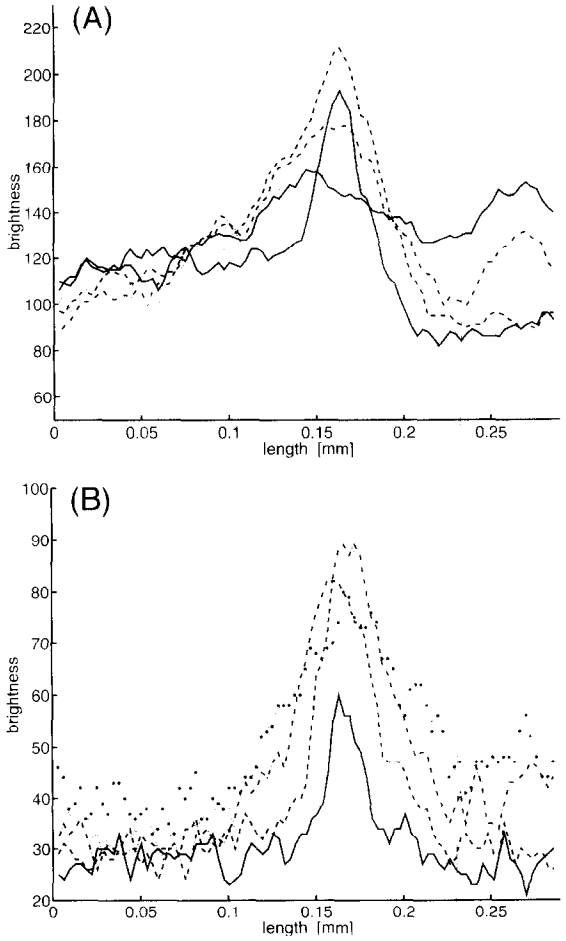

Fig. 13. (A) Evolution of a single LTR cross-section measured with calcein fluorescence. The bottom (on the right side of the graph) curve (—) represents the brightness of an LTR from a skin sample after having been pulsed three times $U_{skin} = 76$ V. The remaining four curves represent the fluorescence of the same LTR and nearby surface after pulsing with progressively higher voltages. From the bottom (on the right side) of the graph up: (—) 78 V, three pulses; (- - -) 78 V, ten pulses and 98 V, three pulses; (- · - · - · -) 78 V ten pulses, 98 V ten pulses, and 118 V, three pulses; ("""") 78 V ten pulses, 98 V ten pulses, and 118 V, ten pulses, and 158 V, three pulses; (—) 78 V ten pulses, 98 V ten pulses, and 118 V, ten pulses, and 158 V, ten pulses. As pulses are applied the fluorescence of the original LTR first increases from (—) to (- - -) but then rapidly diminishes to (- · - · - · -) then ("""") and finally (—). Simultaneously, to the right of the original LTR one observes the evolution of a new LTR with continued pulsing: from (—) to (- - -) to (- · - · - · -) to ("""") and finally to (—). (B) Evolution of the same LTR as in (A) visualized with sulforhodamine. For the meaning of the lines refer to (A). In contrast to the results for calcein, the same original LTR visualized with sulforhodamine increases in fluorescence much more and over a longer course of pulsing: from (—) to (- - - -) to (- · - · - · -) to ("""). It eventually decreases somewhat: from ("""") to (—). There is also the appearance of a new LTR to the right of the original LTR.

LTR making it even less likely that it will reopen.

The fractional area of the pulsed skin preparation covered by LTR's ranged from $2 \cdot 10^{-4}$ (after three pulses at 78 V) to $3.0 \cdot 10^{-2}$ (after ten pulses at 158 V) for sulforhodamine, and from $5 \cdot 10^{-4}$ (after three pulses at 78 V) to $8.2 \cdot 10^{-2}$ (after ten pulses at 158 V) for calcein. These values are significantly more than the fractional area, Fw, we calculated $5 \cdot 10^{-5}$ [18]. This discrepancy can be explained if one assumes that not all of the area of an LTR is involved in transdermal transport, just as in bilayer membrane electroporation [22]. The lateral spreading of LTR's which occurs after a pulse is applied would support this assertion.

Acknowledgements

This work was supported by the Deutsche Forschungsgemeinschaft, NIH Shannon Award ARH4921, and Cygnus Therapeutic Systems, Inc. We thank the group of E.R. Edelman for the use of their video imaging system and M.R. Prausnitz, C. Cullander, R.H. Guy, and H. Boddé for helpful discussions.

References

[1] M.R. Prausnitz, V.G. Bose, R. Langer and J.C. Weaver, Transdermal drug delivery by electroporation, Proc. Int. Symp. Control. Rel. Bioact. Mater., 19 (1992) 232–233.

[2] M.R. Prausnitz, V.G. Bose, R. Langer and J.C. Weaver, Electroporation of mammalian skin: A mechanism to enhance transdermal drug delivery, Proc. Natl. Acad. Sci. USA, 90 (1993) 10504–10508.

[3] T.E. Zewert, U.F. Pliquett, R. Langer and J.C. Weaver, Transport of DNA antisense oligonucleotides across skin by electroporation, Biochem. Biophys. Res. Commun., 212 (1995) 286–292.

[4] D. Bommannan, J. Tamada, L. Leung and R.O. Potts, Effect of electroporation on transdermal iontophoretic delivery of luteinizing hormone releasing hormone (LHRH) in vitro. Pharmacol. Res., 11 (1994) 1809–1814.

[5] M.-R. Riviere, R.A. Rogers, D. Bommannan, J.A. Tamada and R.O. Potts, Pulsatile transdermal delivery of LHRH using electroporation: drug delivery and skin toxicology, J. Controlled Rel., (1995) in press.

[6] U. Pliquett, R. Langer and J.C. Weaver, The change in the passive electrical properties of human stratum corneum due to electroporation, Biochim. Biophys. Acta, (1995) in press.

[7] J.C. Weaver and A. Barnett, Progress towards a theoretical model for electroporation mechanism: membrane electrical behavior and molecular transport, in D.C. Chang, B.M. Chassy, J.A. Saunders and A.E. Sowers (Editors), Guide to Electroporation and Electrofusion, New York, Academic Press, 1992.

[8] J.C. Weaver, Electroporation: a general phenomenon for manipulating cells and tissues, J. Cell. Biochem., 51 (1993) 426–435.

[9] Y.A. Chizmadzhev, V. Zarnystin, J.C. Weaver and R.O. Potts, Mechanism of electroinduced ionic species transport through a multilamellar system, Biophys. J., 68 (1995) 749–765.

[10] S. Grimnes, Pathways of ionic flow through human skin in vivo, Acta Derm. Venereol. (Stockholm), 64 (1984) 93–98.

[11] E.R. Scott, H.S. White and J.B. Phipps, Direct imaging of ionic pathways in stratum corneum using scanning electrochemical microscopy, Solid State Ionics, 53–56 (1992) 176–183.

[12] H.E. Boddé, I. van den Brink, H.K. Koerten and F.H.N. de Haan, Visualization of in vitro percutaneous penetration of mercuric chloride; transport through intercellular space versus cellular uptake through desmosomes, J. Controlled Release, 15 (1991) 227–236.

[13] M.R. Prausnitz, R.H. Guy, R. Langer, J.C. Weaver and C. Cullander, Imaging regions of transport across human stratum corneum during high-voltage and low-voltage exposures, submitted for publication.

[14] C.L. Gummer, The in vitro evaluation of transdermal delivery, in J. Hadgraft and R.H. Guy (Editor), Transdermal drug delivery: development issues and research initiatives, Marcel Dekker, New York, 1989.

[15] R.M. Roberts, J.C. Gilbert, L.B. Rodewald and A.S. Wingrove, Modern Experimental Organic Chemistry, Saunders, Philadelphia, PA, 4th edn., 1985, p. 701.

[16] U. Pliquett and J.C. Weaver, Transport of a charged molecule across the human epidermis due to electroporation, J. Controlled Rel., (1995) in press.

[17] U. Pliquett, M.R. Prausnitz, Y.A. Chizmadzhev and J.C. Weaver, Measurement of rapid release kinetics for transdermal and other types of drug delivery, Pharmacol. Res., 4 (1995) 546–553.

[18] U. Pliquett and J.C. Weaver, Electroporation of human skin: Simultaneous measurement of changes in the transport of two fluorescent molecules and in the passive electrical properties, Bioelectrochem. Bioenerget., (1995) in press.

[19] E.R. Scott, A.I. Laplaza, H.S. White and J.B. Phipps, Transport of ionic species in skin: contribution of pores to the overall skin conductance, Pharmacol. Res., 10 (1993) 1699–1709.

[20] K.T. Powell and J.C. Weaver, Transient aqueous pores in bilayer membranes: a statistical theory, Bioelectrochem. Bioenerg., 15 (1986) 211–227.

[21] A. Barnett and J.C. Weaver, A unified, quantitative theory of reversible electrical breakdown and rupture, Bioelectrochem. Bioenerg., 25 (1991) 163–182.

[22] S.A. Freeman, M.A. Wang and J.C. Weaver, Theory of electroporation of planar membranes: predictions of the aqueous area, change in capacitance and pore-pore separation, Biophys. J., 67 (1994) 42–56.